Digital Repetitive Learning Controller for Three-Phase CVCF PWM Inverter

Keliang Zhou and Danwei Wang, *Member, IEEE*

***Abstract*—In this paper, a plug-in digital repetitive learning control scheme is proposed for three-phase constant-voltage constant-frequency (CVCF) pulsewidth modulation inverters to achieve high-quality sinusoidal output voltages. In the proposed control scheme, the repetitive controller (RC) is plugged into the stable one-sampling-ahead-preview-controlled three-phase CVCF inverter system using only two voltage sensors. The RC is designed to eliminate periodic disturbance and/or track periodic reference signal with zero tracking error. The design theory of plug-in repetitive learning controller is described systematically and the stability analysis of overall system is discussed. The merits of the controlled systems include features of minimized total harmonics distortion, robustness to parameter uncertainties, fast response, and fewer sensors. Simulation and experimental results are provided to illustrate the effectiveness of the proposed scheme.**

***Index Terms*—Pulsewidth modulation inverter, repetitive control.**

I. Introduction

THE constant-voltage constant-frequency (CVCF) pulsewidth modulation (PWM) inverters that are used to convert dc voltage to CVCF sinusoidal voltage are widely employed in uninterrupted power supply and other industry facilities. Total harmonic distortion (THD) is one important index to evaluate the performance of the inverters. The harmonics lead to communication interference, excessive heating in capacitors and transformers, solid-state device malfunctions, and so on. Nonlinear loads and parameter uncertainties, causing periodic tracking error, are major sources of THD in ac power systems.

Over the past decades, the high-precision control of CVCF PWM inverters has attracted much attention [1]. In [2]–[5], a deadbeat controller is designed to force the output voltage track reference sinusoidal voltage. A sliding-mode controller [6], [9]–[11] and a hysteresis controller [7] are proposed to overcome parameter uncertainties and load disturbance. A disturbance observer [8] is adopted to reduce the influence of load disturbance. However, these feedback control schemes do not have memory and any imperfection in performance will be repeated in all following cycles. The repetitive learning control method [12], based on the internal model principle [13], is used to achieve high accuracy in the presence of uncertainties for servomechanism in [14]. In most applications, repetitive control is implemented using digital methods [15], [16]. Applications of discrete-time repetitive controllers (RCs) include robots [17], disc drives [18], the steel casting process [19], satellites [20], etc. An RC is applied in a single-phase PWM inverter with preliminary results [21]–[23].

In this paper, the design of a plug-in discrete-time repetitive learning controller is presented and applied to a three-phase CVCF PWM inverter. The design of a plug-in repetitive learning controller is completely formulated. A plug-in RC is designed for the three-phase CVCF PWM inverter, and stability is analyzed. To show the validity of proposed method, simulation and experimental results are illustrated.

Manuscript received January 9, 2001; revised February 1, 2001. Abstract published on the Internet June 6, 2001.

The authors are with the School of Electrical and Electronics Engineering, Nanyang Technological University, Singapore 639798 (e-mail: klzhou@yahoo.com; edwwang@ntu.edu.sg).

Publisher Item Identifier S 0278-0046(01)06284-0.

II. Design of Discrete-Time RC

In discrete time, a periodic signal with a period N can be generated by a delay chain with a positive feedback loop [as shown in Fig. 1(a)]. Consider the discrete-time repetitive control system shown in Fig. 1(b), where $y_d(z)$ is the reference input signal, $y(z)$ is the output signal, $d(z)$ is the disturbance signal, $e(z)$ is the tracking error signal, $G_s(z)$ is the transfer function of the plant, and $G_r(z)$ is the repetitive signal generator; plug-in RC $G_{rc}(z)$ is the feedforward compensator, and $G_c(z)$ is the conventional feedback controller. $G_c(z)$ is chosen so that the following closed-loop transfer function is asymptotically stable:

$$H(z)=\frac{G_c(z)G_s(z)}{1+G_c(z)G_s(z)}=\frac{z^{-d}B(z^{-1})}{A(z^{-1})}=\frac{z^{-d}B^{+}(z^{-1})B^{-}(z^{-1})}{A(z^{-1})} \tag{1}$$

where d is the known number of pure time step delays, $B^{-}(z^{-1})$ is the uncancelable portion of $B(z^{-1})$, and $B^{+}(z^{-1})$ is the cancelable portion of $B(z^{-1})$.

Based on the internal model principle [13], the zero error tracking of any reference input in the steady state can be achieved if a generator of the reference input is included in the stable closed-loop system. Therefore, for a periodic reference input, the RC $G_{rc}(z)$ is plugged into the system shown in Fig. 1 as follows [15]:

$$G_{rc}(z)=G_r(z)G_f(z)=\frac{k_r z^{-N}}{1-z^{-N}}G_f(z) \tag{2}$$

where the repetitive signal generator $G_r(z)$ and the filter $G_f(z)$ are chosen as follows:

$$G_r(z)=\frac{k_r z^{-N}}{1-z^{-N}}=\frac{k_r}{z^N-1} \tag{3}$$

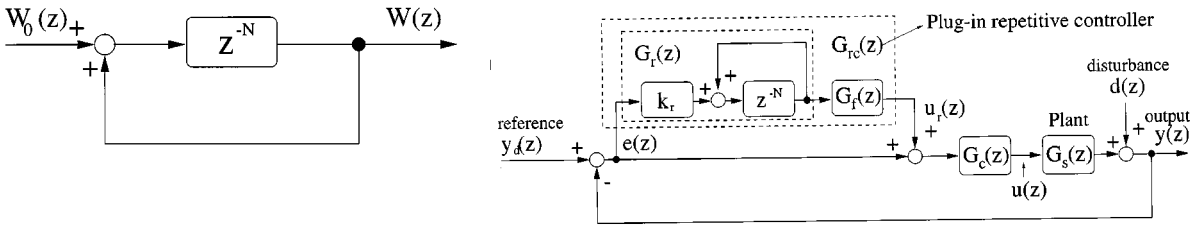

(a) (b)

Fig. 1. Repetitive control system. (a) Periodic signal generator. (b) Plug-in repetitive control system.

$$G_f(z) = \frac{z^{-n_u} A(z^{-1}) B^-(z)}{B^+(z^{-1}) b} \tag{4}$$

where k_r is the *repetitive control gain*, $N = f/f_c$ with f being the reference signal frequency and f_c being the sampling frequency, $B^-(z)$ is obtained from $B^-(z^{-1})$ with z^{-1} replaced by z, b is a scalar chosen so that $b \geq [B^-(1)]^2$ n_u is the order of $B^-(z^{-1})$, and z^{-n_u} makes the filter realizable. $G_f(z)$ in (4) is an implementation of the *zero phase error tracking controller* design [24].

From Fig. 1, the transfer functions from $y_d(z)$ and $d(z)$ to $y(z)$ in the overall closed-loop system are respectively, derived, as

$$\begin{aligned} \frac{y(z)}{y_d(z)} &= \frac{\left(1 + G_r(z)G_f(z)\right) G_c(z)G_s(z)}{1 + \left(1 + G_r(z)G_f(z)\right) G_c(z)G_s(z)} \\ &= \frac{\left(1 - z^{-N} + k_r z^{-N} G_f(z)\right) H(z)}{1 - z^{-N}\left(1 - k_r G_f(z)H(z)\right)} \end{aligned} \tag{5}$$

$$\begin{aligned} \frac{y(z)}{d(z)} &= \frac{1}{1 + G_c(z)G_s(z)} \left(1 - z^{-N}\right) \\ &\quad \cdot \frac{1}{1 - z^{-N}\left(1 - k_r G_f(z)H(z)\right)} \end{aligned} \tag{6}$$

and the error transfer function for the overall system is

$$\begin{aligned} G_e(z) = \frac{e(z)}{y_d(z) - d(z)} &= \frac{1}{1 + G_c(z)G_s(z)} \left(1 - z^{-N}\right) \\ &\quad \cdot \frac{1}{1 - z^{-N}\left(1 - k_r G_f(z)H(z)\right)}. \end{aligned} \tag{7}$$

From (1) and (5)–(7), it can be concluded that the overall closed-loop system is stable if the following two conditions hold:

1) the roots of $1 + G_c(z)G_s(z) = 0$ are inside the unit circle;
2)

$$\left\| 1 - k_r G_f(z)H(z) \right\| < 1, \qquad \text{for } z = e^{j\omega},\ 0 < \omega < \frac{\pi}{T}. \tag{8}$$

Obviously, if the overall closed-loop system shown in Fig. 1 is asymptotically stable and the angular frequency ω of the reference input $y_d(t)$ and the disturbance $d(t)$ approaches $\omega_m = 2\pi m f$, $m = 0, 1, 2, \ldots, M$ ($M = N/2$ for even N and $M = (N-1)/2$ for odd N), then $z^{-N} \to 1$, $\lim_{\omega \to \omega_m}$, $\|G_e(j\omega)\| = 0$ and, thus,

$$\lim_{\omega \to \omega_m} \|e(j\omega)\| = 0. \tag{9}$$

Equation (9) implies that zero steady-state error is obtained with repetitive learning control for any periodic disturbance or reference whose frequency is less than half of the sampling frequency.

Because the open-loop poles of the repetitive learning controller are on the stability boundary, the stability of the overall system is sensitive to unmodeled dynamics [17]. In order to enhance the robustness of the system, a low-pass filter $Q(z, z^{-1})$ [17] is used in the repetitive learning controller as follows:

$$G_r(z) = \frac{k_r Q(z, z^{-1}) z^{-N}}{1 - Q(z, z^{-1}) z^{-N}} \tag{10}$$

where

$$Q(z, z^{-1}) = \frac{\sum_{i=0}^{m} \alpha_i z^i + \sum_{i=1}^{m} \alpha_i z^{-i}}{2\sum_{i=1}^{m} \alpha_i + \alpha_0} \tag{11}$$

where α_i ($i = 0, 1, \ldots, m$; $m = 0, 1, 2, \ldots, N/2$) are coefficient to be designed.

Notice that $Q(z, z^{-1})$ is a moving average filter that has zero phase shift and bring all open-loop poles inside the unit circle except the one at $+1$. A first order filter $Q(z, z^{-1}) = (z + 2 + z^{-1})/4$ is generally sufficient. On the other hand, high frequency periodic disturbance are not perfectly canceled by this controller. In this case, a tradeoff is made between tracking precision and system robustness [25]. And correspondingly, equation (8) is conservatively modified as follows [18]:

$$\left\| 1 - k_r G_f(z)H(z) \right\| < 1 \leq \left\| \frac{1}{Q(z, z^{-1})} \right\|. \tag{12}$$

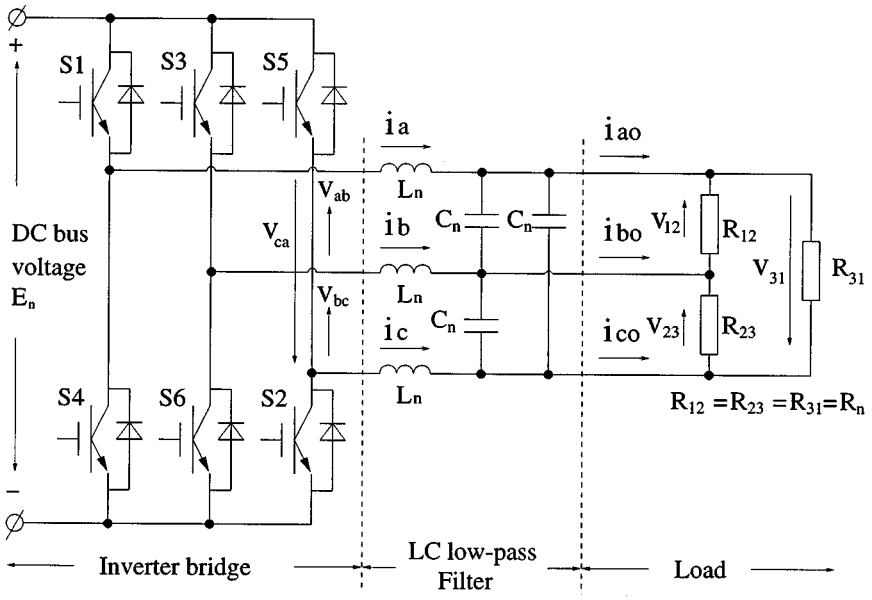

Fig. 2. Three-phase CVCF PWM inverter with nominal parameters.

III. Repetitive-Controlled Three-Phase CVCF PWM Inverter

A. Modeling Three-Phase CVCF PWM Inverter

The electrical dynamics of a three-phase PWM inverter as shown in Fig. 2 can be described as follows [8]:

$$\begin{pmatrix} 1 & 0 & -1 & 0 & 0 & 0 \\ -1 & 1 & 0 & 0 & 0 & 0 \\ 0 & -1 & 1 & 0 & 0 & 0 \\ 0 & 0 & 0 & 1 & -1 & 0 \\ 0 & 0 & 0 & 0 & 1 & -1 \\ 0 & 0 & 0 & -1 & 0 & 1 \end{pmatrix} \begin{pmatrix} \dot{v}_{12} \\ \dot{v}_{23} \\ \dot{v}_{31} \\ \dot{i}_a \\ \dot{i}_b \\ \dot{i}_c \end{pmatrix}$$

$$= \begin{pmatrix} \frac{-1}{R_nC_n} & 0 & \frac{1}{R_nC_n} & \frac{1}{C_n} & 0 & 0 \\ \frac{1}{R_nC_n} & \frac{-1}{R_nC_n} & 0 & 0 & \frac{1}{C_n} & 0 \\ 0 & \frac{1}{R_nC_n} & \frac{-1}{R_nC_n} & 0 & 0 & \frac{1}{C_n} \\ \frac{-1}{L_n} & 0 & 0 & 0 & 0 & 0 \\ 0 & \frac{-1}{L_n} & 0 & 0 & 0 & 0 \\ 0 & 0 & \frac{-1}{L_n} & 0 & 0 & 0 \end{pmatrix} \begin{pmatrix} v_{12} \\ v_{23} \\ v_{31} \\ i_a \\ i_b \\ i_c \end{pmatrix}$$

$$+ \begin{pmatrix} 0 & 0 & 0 \\ 0 & 0 & 0 \\ 0 & 0 & 0 \\ \frac{1}{L_n} & 0 & 0 \\ 0 & \frac{1}{L_n} & 0 \\ 0 & 0 & \frac{1}{L_n} \end{pmatrix} \begin{pmatrix} v_{ab} \\ v_{bc} \\ v_{ca} \end{pmatrix} \tag{13}$$

where the output line-to-line voltages v_{12}, v_{23}, and v_{31} and phase currents i_a, i_b, and i_c are state variables, PWM modulated voltages $v_{ab} = E_n \Delta T_{ab}$, $v_{bc} = E_n \Delta T_{bc}$, and $v_{ca} = E_n \Delta T_{ca}$ are control inputs, and ΔT_{ab}, ΔT_{bc}, and ΔT_{ca} are the corresponding pulsewidths in one sampling interval, E_n is the nominal dc-bus voltage, and $L_n(>0)$, $C_n(>0)$, and $R_n(>0)$ are the nominal values of the inductor, capacitor and resistant load, respectively.

Through 3/2 and 2/3 transformations between (a, b, c), and (α, β) [26], (13) can be transformed into

$$\begin{pmatrix} \dot{v}_\alpha \\ \dot{i}_\alpha \\ \dot{v}_\beta \\ \dot{i}_\beta \end{pmatrix} = \begin{pmatrix} \frac{-1}{R_nC_n} & \frac{1}{3C_n} & 0 & 0 \\ \frac{-1}{L_n} & 0 & 0 & 0 \\ 0 & 0 & \frac{-1}{R_nC_n} & \frac{1}{3C_n} \\ 0 & 0 & \frac{-1}{L_n} & 0 \end{pmatrix} \begin{pmatrix} v_\alpha \\ i_\alpha \\ v_\beta \\ i_\beta \end{pmatrix}$$

$$+ \begin{pmatrix} 0 & 0 \\ \frac{E_n}{L_n} & 0 \\ 0 & 0 \\ 0 & \frac{E_n}{L_n} \end{pmatrix} \begin{pmatrix} \Delta T_\alpha \\ \Delta T_\beta \end{pmatrix}. \tag{14}$$

Equation (14) indicates that the two-phase system can be decoupled into two identical independent single-phase systems as follows:

$$\begin{pmatrix} \dot{x}_1 \\ \dot{x}_2 \end{pmatrix} = \begin{pmatrix} \frac{-1}{R_nC_n} & \frac{1}{3C_n} \\ \frac{-1}{L_n} & 0 \end{pmatrix} \begin{pmatrix} x_1 \\ x_2 \end{pmatrix} + \begin{pmatrix} 0 \\ \frac{E_n}{L_n} \end{pmatrix} u \tag{15}$$

where $x_1 = v_\alpha$ or v_β, $x_2 = i_\alpha$ or i_β, and $u = \Delta T_\alpha$ or ΔT_β.

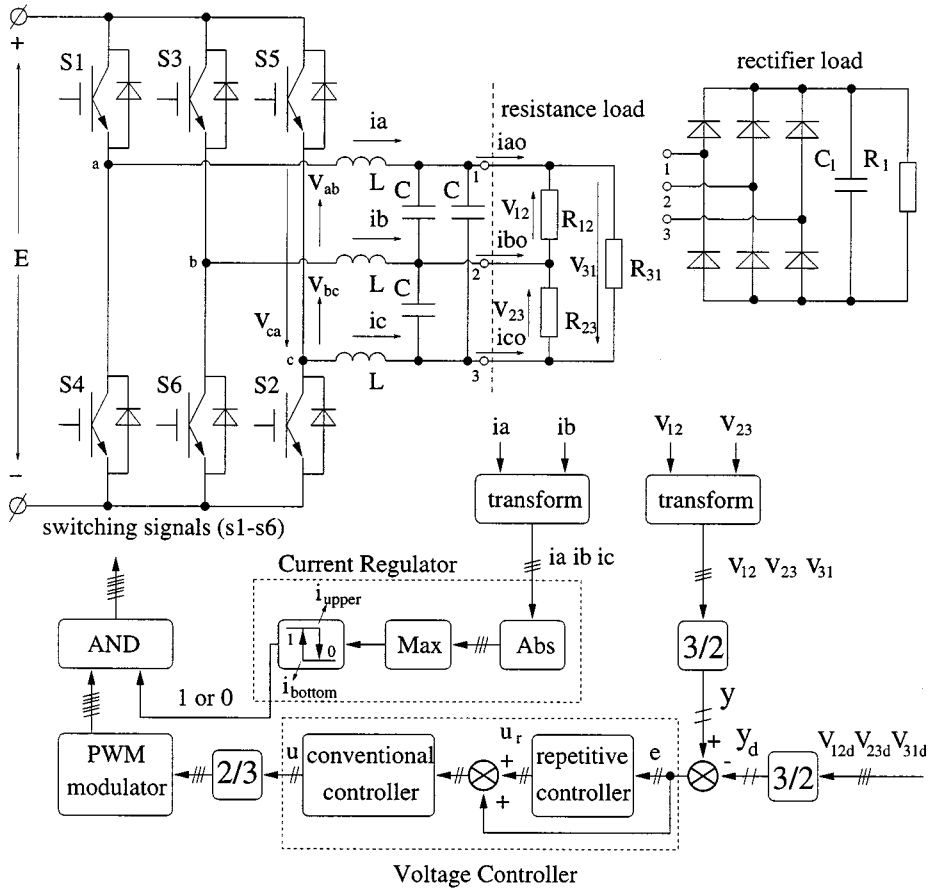

Fig. 3. Controlled three-phase PWM inverter.

For a linear system $\dot{\mathbf{x}} = A\mathbf{x} + B\mathbf{u}$, its sampled-data equation can be expressed as $\mathbf{x}(k+1) = e^{AT}\mathbf{x}(k) + \int_0^T e^{AT-\tau)}B\mathbf{u}(\tau)\,d\tau$. Therefore, a sampled-data form for (15) can be derived as follows:

$$\begin{pmatrix} x_1(k+1) \\ x_2(k+1) \end{pmatrix} = \begin{pmatrix} \varphi_{11} & \varphi_{12} \\ \varphi_{21} & \varphi_{22} \end{pmatrix} \begin{pmatrix} x_1(k) \\ x_2(k) \end{pmatrix} + \begin{pmatrix} g_1 \\ g_2 \end{pmatrix} u(k) \tag{16}$$

where

$$\varphi_{11} = 1 - \frac{T}{C_n R_n} + \frac{T^2}{2C_n^2 R_n^2} - \frac{T^2}{6L_n C_n}$$

$$\varphi_{12} = \frac{T}{3C_n} - \frac{T^2}{6C_n^2 R_n}$$

$$\varphi_{21} = -\frac{T}{L_n} + \frac{T^2}{2L_n C_n R_n}$$

$$\varphi_{22} = 1 - \frac{T^2}{6L_n C_n},$$

$$g_1 = \frac{E_n T}{6L_n C_n}$$

$$g_2 = \frac{E_n}{L_n}.$$

B. Problem Description

Consider a three-phase CVCF PWM inverter described by (16) and the following discrete-time output equation:

$$y(k) = x_1(k). \tag{17}$$

Given desirable trajectory $y_d(k)$ being a periodic function, i.e., $y_d(k+N) = y_d(k)$, where the period of $y_d(k)$ is $N*T$, we are to design a feedback controller and a plug-in RC to achieve, in the presence of uncertainties and disturbance,

$$\lim_{i\to\infty} ||y_d(k) - y(k+i*N)|| \to 0. \tag{18}$$

In other words, the objective is to force v_{12}, v_{23}, and v_{31} track v_{12d}, v_{23d}, and v_{31d} with zero error at the sampling points.

C. Design of Digital Controller

According the theory in Section II, the digital controller for three-phase CVCF PWM inverter is comprised of two parts: a conventional feedback controller and a plug-in RC.

1) Conventional Feedback Controller: The ARMA equation for the dynamics (16) and (17) can be obtained as follows:

$$y(k+1) = -p_1 y(k) - p_2 y(k-1) + m_1 u(k) + m_2 u(k-1) \tag{19}$$

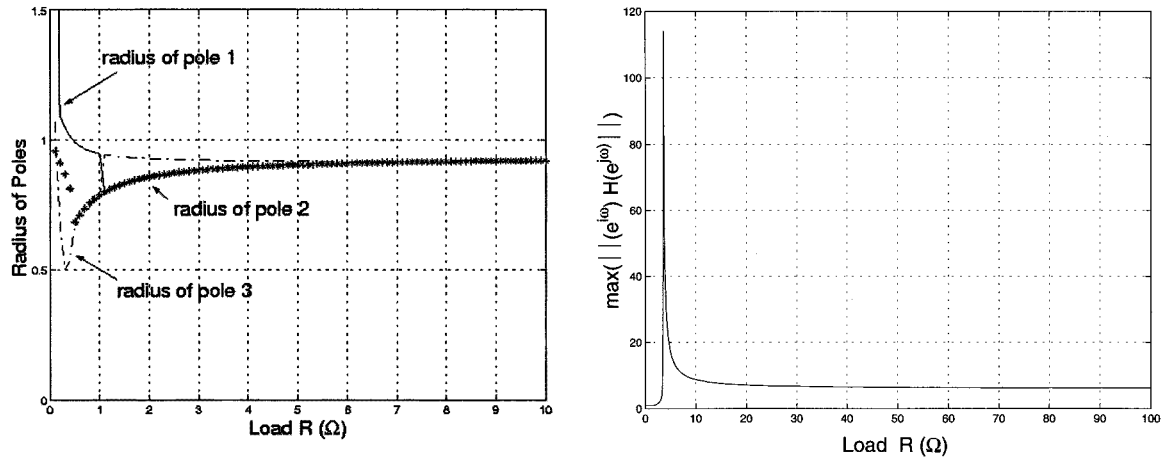

(a) (b)

Fig. 4. Stability analysis. (a) Radius of poles of $H(z)$. (b) Maximum $\|e^{j\omega}H(e^{j\omega})\|$.

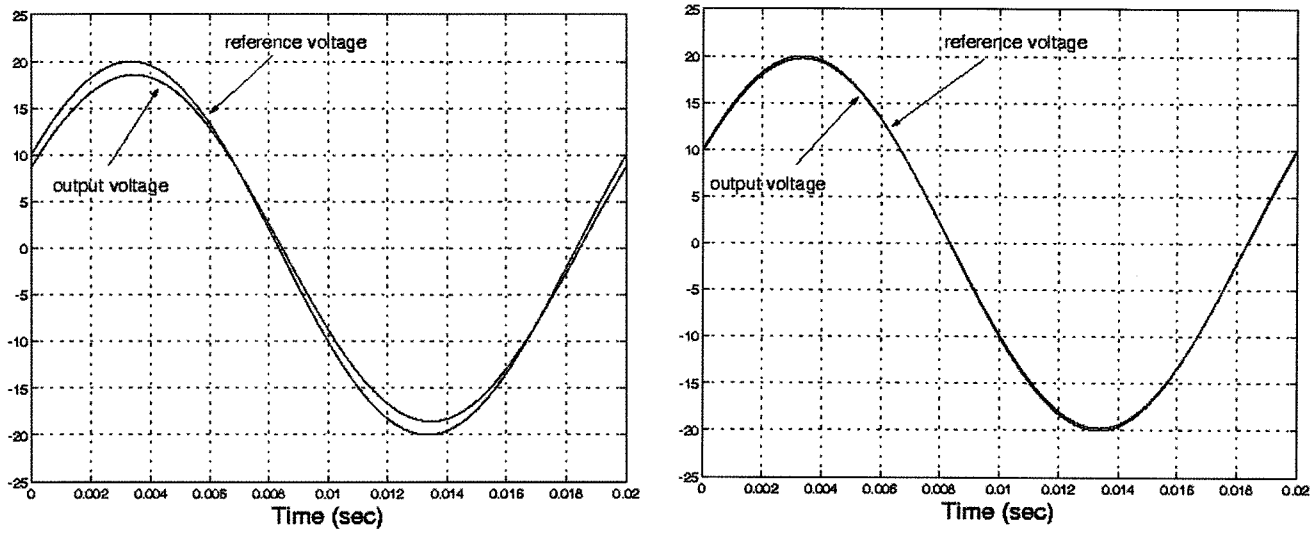

(a) (b)

Fig. 5. Simulated steady-state response under no load. (a) OSAP-controlled $v_{12\,d}$, v_{12}. (b) OSAP + RC-controlled $v_{12\,d}$, v_{12}.

where

$$\begin{aligned} u(k) &= \pm\Delta T(k) \\ p_1 &= -(\varphi_{11}+\varphi_{22}) \\ p_2 &= \varphi_{11}\varphi_{22}-\varphi_{21}\varphi_{12} \\ m_1 &= g_1 \\ m_2 &= g_2\varphi_{12}-g_1\varphi_{22}. \end{aligned}$$

If the control law for the plant (19) is chosen as follows:

$$u(k) = \frac{1}{m_1}\left[y_d(k) - m_2u(k-1) + p_1y(k) + p_2y(k-1)\right] \tag{20}$$

then it yields deadbeat response $y(k+1) = y_d(k)$ with transfer function as $H_n(z) = z^{-1}$. The feedback controller in (20) is called the *one-sampling-ahead preview* (OSAP) controller [2].

2) Plug-In RC: In addition to a sampling time tracking error, OSAP controllers depend on the accuracy of the model parameters. In practice, load disturbances ΔR, parameter uncertainties ΔL and ΔC, and dc-bus voltage disturbance ΔE lead to large tracking errors. Then, a repetitive learning controller can be applied to overcome the periodic disturbance and parameter variations. According to the repetitive learning control mentioned in Section II, the RC is proposed as follows:

$$G_{rc}(z) = G_r(z)G_f(z) = \frac{k_rz^{-N+1}Q(z,\, z^{-1})}{1 - Q(z,\, z^{-1})z^{-N}}. \tag{21}$$

In order to enhance the robustness, $Q(z, z^{-1})$ can be set as $d_1z + d_0 + d_1z^{-1}$, where $2d_1 + d_0 = 1$. If $Q(z, z^{-1}) = 1$, in sampled-data form, the RC (21) can be expressed as follows:

$$u_r(k) = u_r(k-N) + k_re(k-N+1). \tag{22}$$

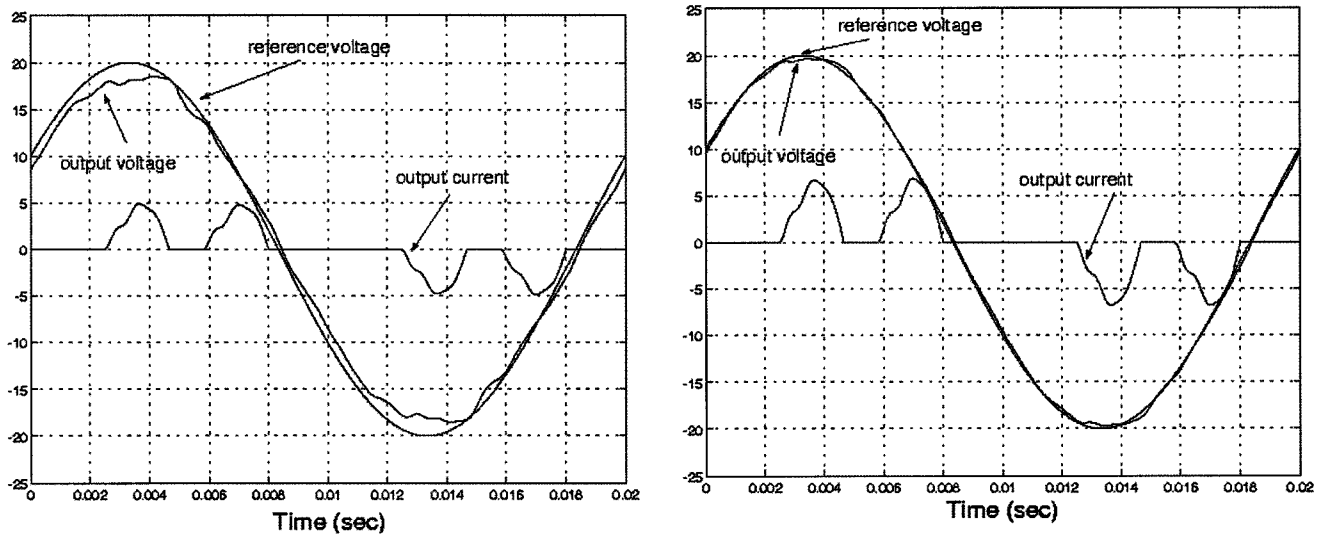

(a) (b)

Fig. 6. Simulated steady-state response under uncontrolled rectifier load. (a) OSAP-controlled $v_{12\,d}$, v_{12}. (b) OSAP + RC-controlled $v_{12\,d}$, v_{12}, i_{ao}.

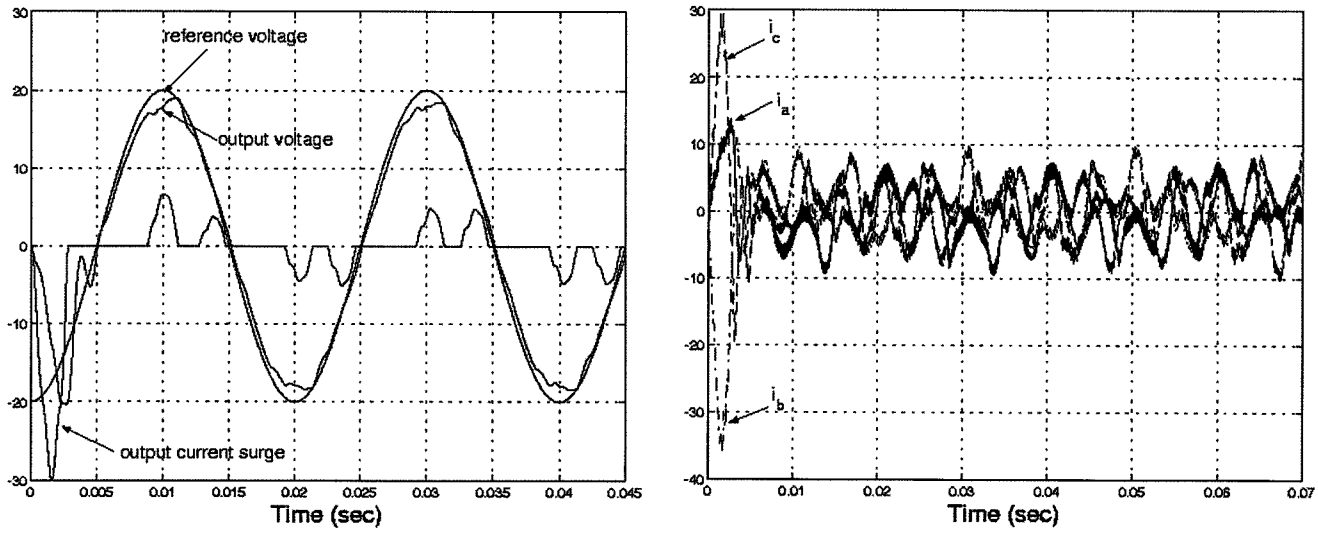

(a) (b)

Fig. 7. Simulated OSAP + RC-controlled transient responses without current regulator. (a) Transient response $v_{12\,d}$, v_{12}, i_{ao}. (b) Transient response i_a, i_b, i_c.

In fact, (22) is the same as an anticipatory learning control law [27].

D. Robustness Analysis

With the presence of the uncertainties ΔL, ΔC, ΔR, and ΔE, the ARMA equation for the actual plant becomes

$$y(k+1) = -a_1 y(k) - a_2 y(k-1) + b_1 u(k) + b_2 u(k-1) \quad (23)$$

where $a_1 = p_1 + \Delta p_1$, $a_2 = p_2 + \Delta p_2$, $b_1 = m_1 + \Delta m_1$, and $b_2 = m_2 + \Delta m_2$ are calculated on the basis of the practical parameters $L = L_n + \Delta L$, $C = C_n + \Delta C$, $E = E_n + \Delta E$, and $R = R_n + \Delta R$.

Therefore, when the OSAP controller (20) is applied to the plant (23), the closed-loop transfer function $H(z)$ without RC controller becomes

$$H(z) = \frac{(b_1 + b_2 z^{-1})}{(z + a_1 + a_2 z^{-1})(m_1 + m_2 z^{-1}) - (p_1 + p_2 z^{-1})(b_1 + b_2 z^{-1})}. \quad (24)$$

According to the stability analysis in Section II, the overall system is stabilized if:

1) all poles of $H(z)$ in (24) are inside the unit circle;
2) $||1 - k_r z H(z)|| < 1 \le (1/(||Q(z, z^{-1})||))$, where k_r can be larger due to the introduction of $Q(z, z^{-1})$.

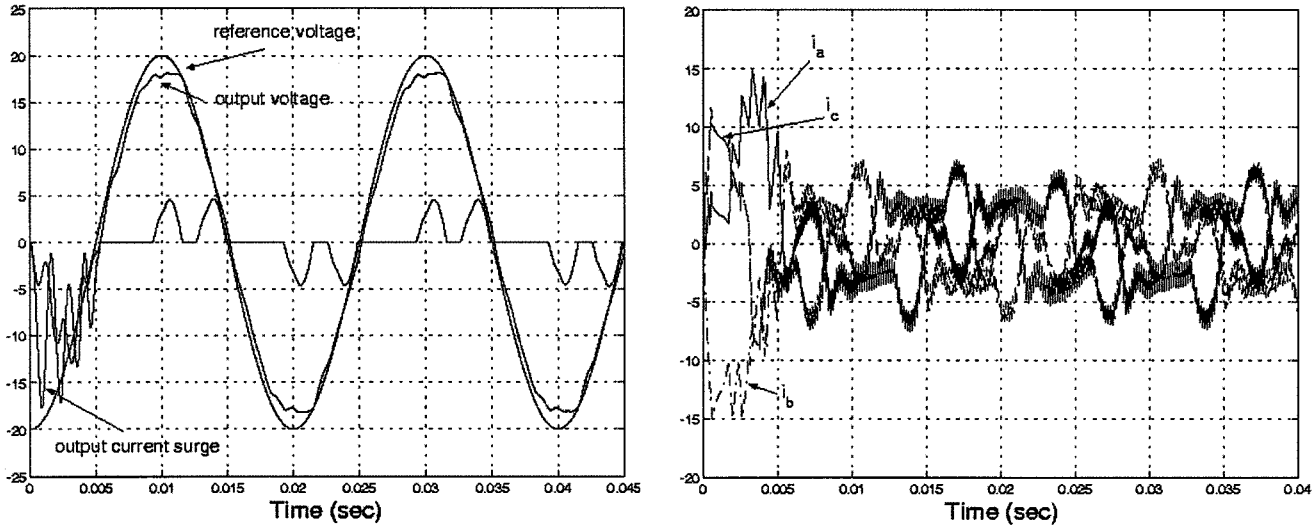

(a) (b)

Fig. 8. Simulated OSAP + RC-controlled transient responses with current regulator. (a) Transient response $v_{12\,d}$, v_{12}, i_{ao}. (b) Transient response i_a, i_b, i_c.

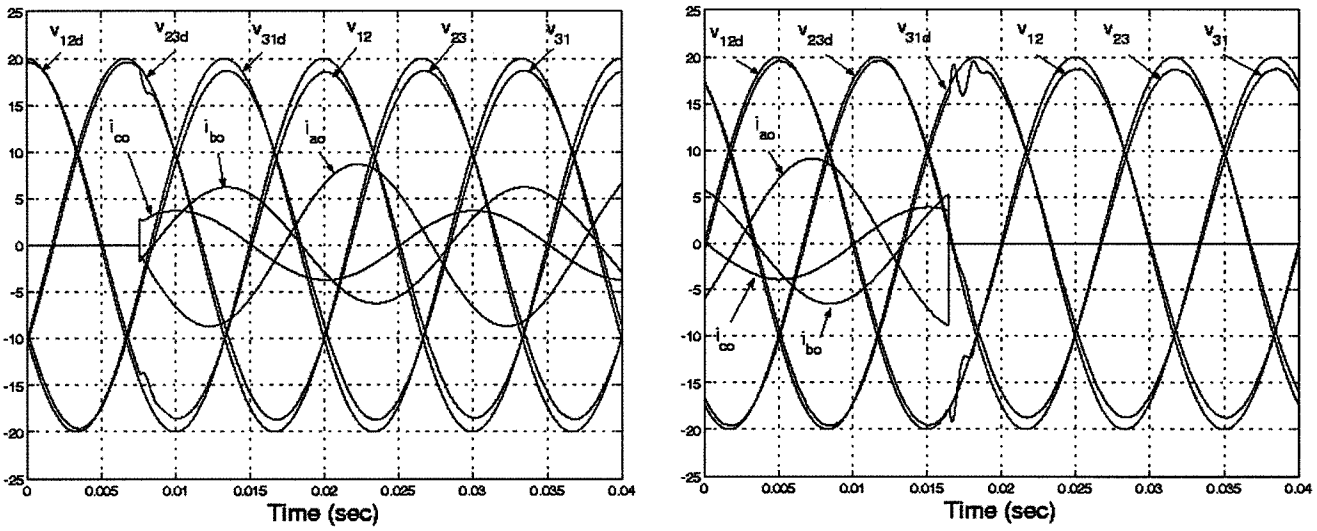

(a) (b)

Fig. 9. Simulated OSAP + RC-controlled transient responses under sudden load changes. (a) Transient response $v_{12\,d}$, v_{12}, i_{ao} under sudden load change (from $R_{12} = R_{23} = R_{31} = \infty\ \Omega$ to $R_{12} = 3\ \Omega$, $R_{23} = 5\ \Omega$, $R_{31} = \infty\ \Omega$). (b) Transient response $v_{12\,d}$, v_{12}, i_{ao} under sudden load change (from $R_{12} = 3\ \Omega$, $R_{23} = 5\ \Omega$, $R_{31} = \infty\ \Omega$ to $R_{12} = R_{23} = R_{31} = \infty\ \Omega$).

E. Simulation and Experiment

All the simulation and experimental studies are carried out using the three-phase PWM inverter system as shown in Fig. 3.

The following parameters are used for simulations and experiments: $E_n = 100$ V, $C_n = 600\ \mu$F, $L_n = 700\ \mu$H, $R_n = 3\ \Omega$; $C = 500\ \mu$F, $L = 600\ \mu$H, $E = 30$ V; v_{12d}, v_{23d}, and v_{31d} are $f = 50$-Hz 20-V peak three-phase sine voltages; sampling and switching frequency $f_c = 1/T = 6.25$ kHz; $N = f/f_c = 125$; and $d_0 = 0.9$, $d_1 = 0.05$.

As shown in Fig. 4(a), with these above parameter values and when $R > 0.4\ \Omega$, all the poles of the closed-loop transfer function $H(z)$ in (24) without RC are located inside the unity circle, the system is stable.

As shown in Fig. 4(b), the maximum gain of $zH(z)$ in the frequency domain is no more than 116. According to the sta-

Fig. 10. Experimental setup.

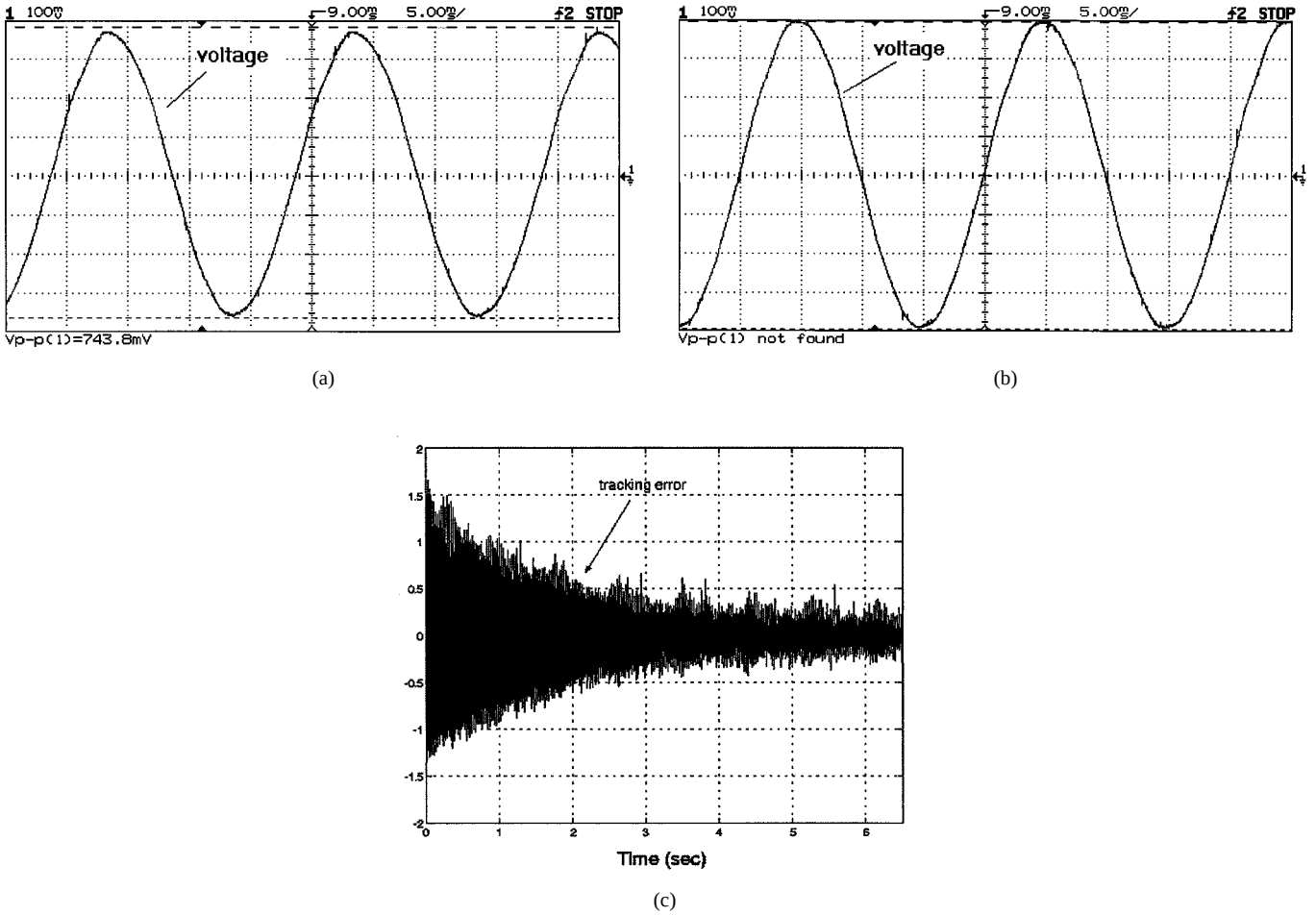

Fig. 11. Experimental results with balanced resistance load. (a) OSAP-controlled steady-state response v_{12} (5 V/div). (b) OSAP + RC-controlled steady-state response v_{12} (5 V/div). (c) OSAP + RC-controlled transient tracking error $e(t) = v_{12\,d}(t) - v_{12}(t)$ (horizontal: 1 s/div; vertical: 0.5 V/div).

bility condition $||1 - k_r z H(z)|| < 1$ for repetitive control design, the system with RC is stable if $k_r \in (0, 0.017)$. We choose $k_r = 0.005$.

Under some transient cases, such as plug-in of rectifier load, overcurrent might occur. Without an internal current regulator, the power switches should be shut down when the transient overcurrent flowing through switches is detected, and then the whole inverter system stops working. In practice, in order to overcome the transient overcurrent, an internal hysteresis current regulator is used. If any one peak of inductor currents i_a, i_b, and i_c exceeds an upper threshold value $i_{\rm upper}$, all the PWM control inputs will be dynamically turned off; if all the peaks of i_a, i_b, and i_c drops to be less than a lower threshold value i_{bottom}, all the PWM control input will be turned on immediately. Hence, the currents that flow through power switches will be limited by the threshold value $i_{\rm upper}$. In our simulations and experiments, $i_{\rm upper} = 15$ A and $i_{\rm bottom} = 10$ A.

1) Simulation Results: Figs. 5 and 6 show the simulation results of the OSAP-controlled and RC + OSAP-controlled three-phase PWM inverters under no load ($R_{12} = R_{23} = R_{31} = \infty\ \Omega$) and uncontrolled rectifier load ($C_1 = 2$ mF, $R_1 = 9.4\ \Omega$), respectively. It is obviously shown that the RC forces the output line-to-line voltage to approach the reference line-to-line voltage under different loads and significantly reduces the tracking error, respectively.

Figs. 7 and 8 show the simulation results of the OSAP + RC-controlled transient responses with/without internal current regulator when an uncontrolled rectifier load ($C_1 = 2$ mF, $R_1 = 9.4\ \Omega$) is plugged in. Without an internal current regulator, the output transient current i_{ao} surges to 30 A and the peak of inductor currents reaches 35 A; with an internal current regulator, the output transient current i_{ao} drops to 18 A and the peak of inductor currents is restricted to be less than 15 A. Obviously, the internal current regulator can successfully overcome the transient overcurrents. Moreover, the system is robust to the transient current surge.

Fig. 9 shows the simulation results of the OSAP + RC-controlled transient responses under sudden load changes between $R_{12} = 3\ \Omega$, $R_{23} = 5\ \Omega$, $R_{31} = \infty\ \Omega$, and $R_{12} = R_{23} = R_{31} = \infty\ \Omega$). It can be seen that the controlled inverter is also robust to sudden load variations.

2) Experimental Results: An experimental setup, as shown in Fig. 10, has been built for the converter system shown in Fig. 3. Dead time for insulated gate bipolar transistor (IGBT) power switches is 3 μs. The OSAP plus repetitive PWM control is implemented in a DSPACE (DS1102) digital

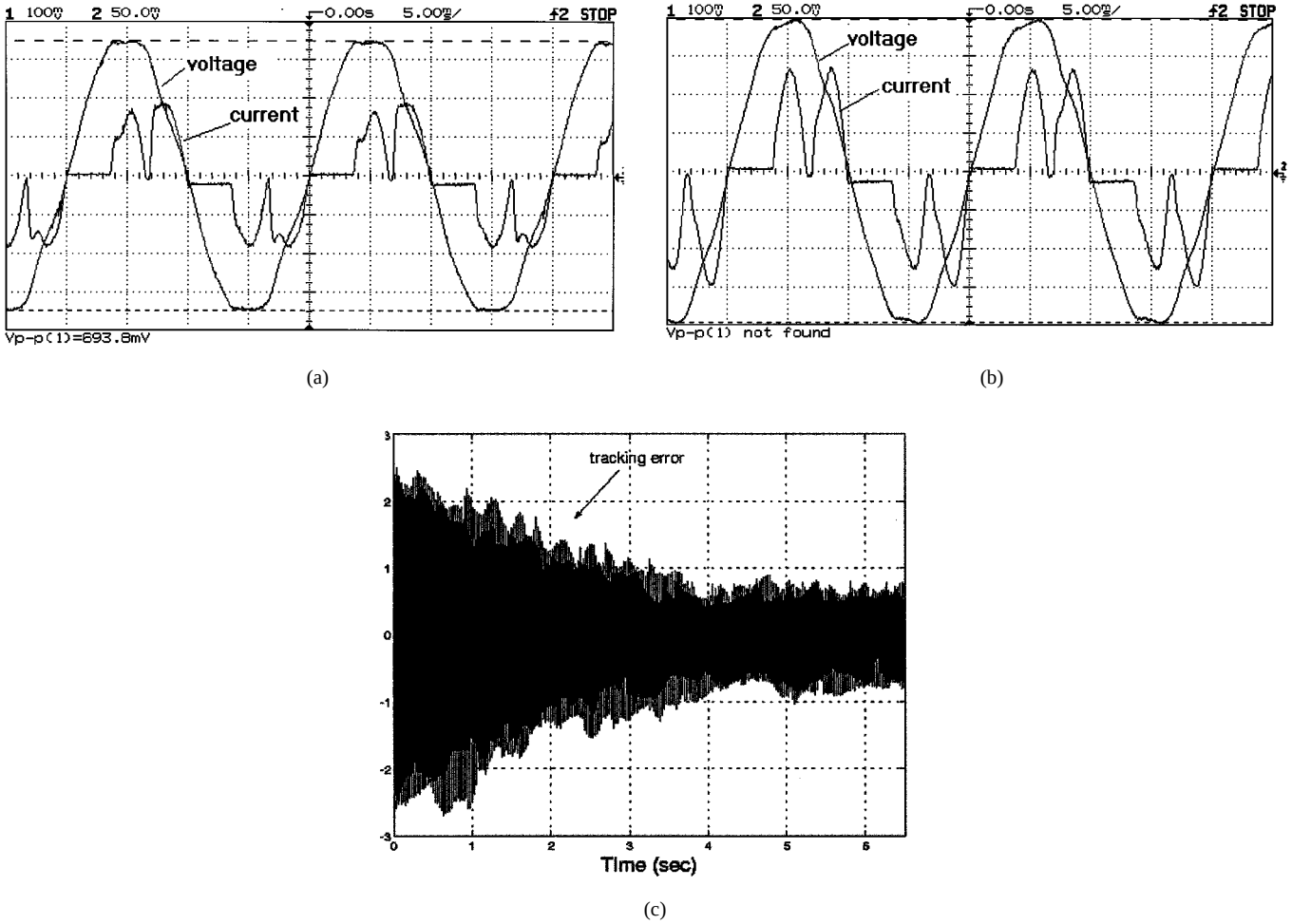

Fig. 12 Experimental results with uncontrolled rectifier load. (a) OSAP-controlled steady-state response v_{12} (5 V/div) and i_{ao} (2.5 A/div). (b) OSAP + RC-controlled steady-state response v_{12} (5 V/div) and i_{ao} (2.5 A/div). (c) OSAP + RC-controlled transient tracking error $e(t) = v_{12\,d}(t) - v_{12}(t)$ (horizontal: 1 s/div; vertical: 1 V/div).

signal processor (DSP) system which results in about 70-μs computational delay. In the proposed control scheme, only two voltage sensors and two current sensors are used for the experiment.

Fig. 11 shows the experimental results of the OSAP and OSAP- + RC-controlled three-phase CVCF PWM inverters under balanced load ($R_{12} = R_{23} = R_{31} = \infty\ \Omega$). Output line-to-line voltage v_{12} is about 18.6-V sine wave with the OSAP controller in Fig. 11(a); output voltage approaches 20-V sine wave with the OSAP + RC controller in Fig. 11(b). Furthermore, Fig. 11(c) shows the tracking error $e(t) = v_{12d} - v_{12}$ is reduced from about 1.4 V to be less than 0.3 V after about 4 s when the RC controller is plugged into the OSAP-controlled inverter.

Fig. 12 shows the experimental results of the OSAP- and OSAP + RC-controlled inverters under uncontrolled rectifier load ($C_1 = 2000\ \mu$F, $R_1 = 9.4\ \Omega$). The OSAP-controlled output line-to-line voltage v_{12} is about 17.3-V sine wave and is distorted by a current surge in Fig. 12(a); the OSAP + RC-controlled output voltage approaches 20-V sine wave and has less distortion with the OSAP + RC controller in Fig. 12(b). Fig. 12(c) shows the peak of tracking error $e(t)$ is reduced from about 2.7 V to be less than 0.8 V after about 4 s when the RC controller is plugged into the OSAP-controlled inverter.

Fig. 13 shows the experimental results of the OSAP- and OSAP + RC-controlled inverters under unbalanced load ($C_1 = 2000\ \mu$F, $R_1 = 9.4\ \Omega$), where an uncontrolled rectifier load ($C_1 = 2000\ \mu$F, $R_1 = 9.4\ \Omega$) is connected between ports 1, 2, and 3 and is left open circuited. It is observed from the experimental result that the plug-in RC successfully forces the peak of tracking error $e(t) = v_{12d} - v_{12}$ from about 1.5 V to be less than 0.6 V under unbalanced load, and the distortion caused by the current surge is also reduced significantly.

In fact, almost identical responses for other output line-to-line voltages v_{23} and v_{31} are obtained in the experiments. Also, it should be pointed out that the residue tracking errors can be reduced further by increasing the sampling frequency f_c.

IV. Conclusion

In this paper, a plug-in discrete-time repetitive learning controller was designed for the three-phase CVCF PWM inverters to achieve high-quality sinusoidal output voltages. Only two voltage sensors and two current sensors are used. It is shown

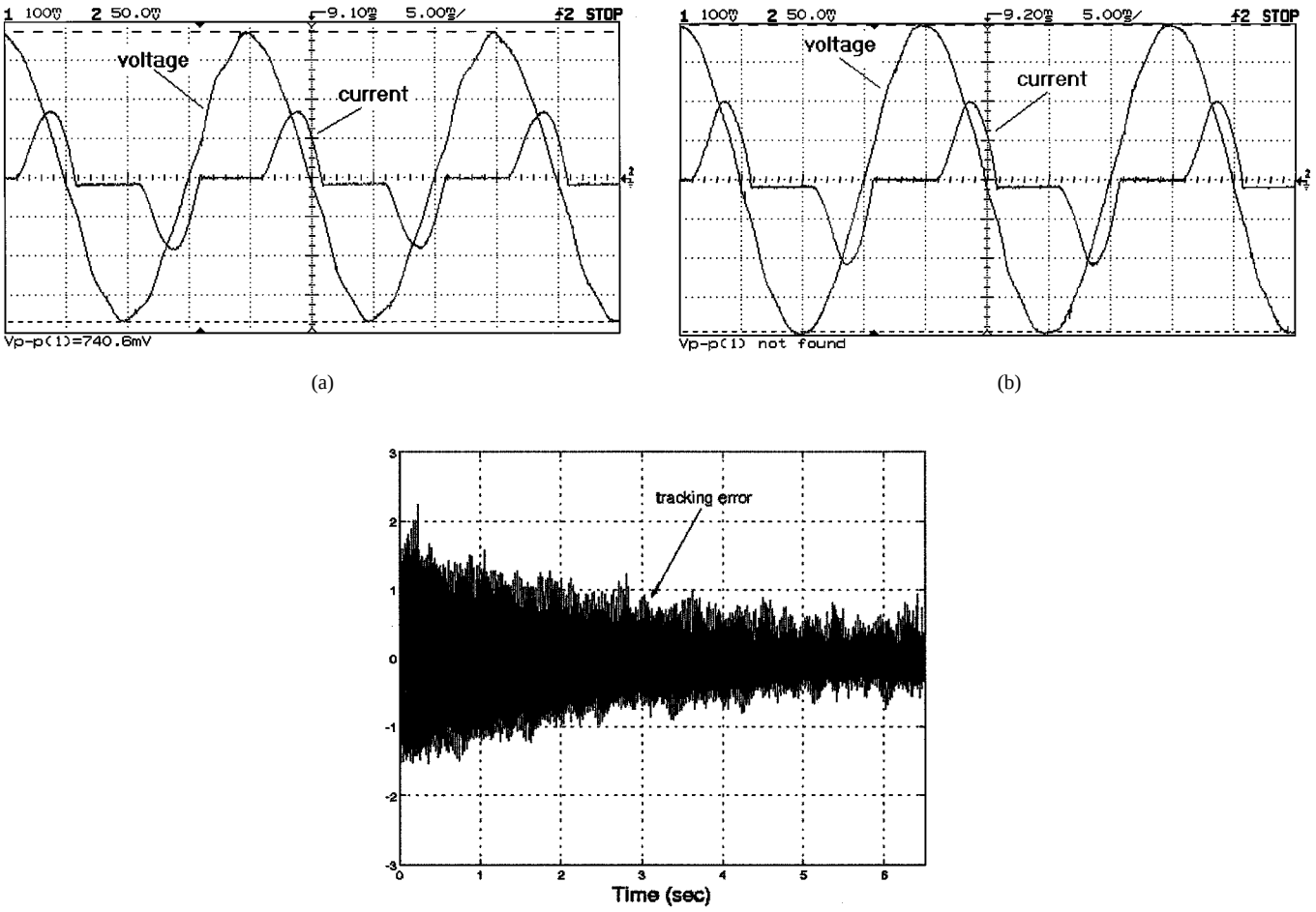

Fig. 13. Experimental results with unbalanced load. (a) OSAP-controlled steady-state response v_{12} (5 V/div) and i_{ao} (2.5 A/div). (b) OSAP + RC-controlled steady-state response v_{12} (5 V/div) and i_{ao} (2.5 A/div). (c) OSAP + RC-controlled transient tracking error $e(t) = v_{12\,d}(t) - v_{12}(t)$ (horizontal: 1 s/div; vertical: 1 V/div).

that the periodic tracking errors caused by parameter uncertainties (ΔL and ΔC), nonlinear load disturbances (such as rectifier load), and dc-bus voltage deviation ΔE are eliminated by the plug-in RC. Moreover, the proposed control scheme possesses the robustness properties to large disturbances and parameter variations and offers less output voltage THD. Simulation and experimental results were provided to validate the proposed control scheme.

REFERENCES

[1] A. Kawamura and T. Yokoyama, "Comparison of five different approaches for real time digital feedback control of PWM inverters," in *Proc. IEEE PESC'90*, 1990, pp. 1005–1011.

[2] A. Kawamura, T. Haneyoshi, and R. G. Hoft, "Deadbeat controlled PWM inverter with parameters estimation using only voltage sensor," *IEEE Trans. Power Electron.*, vol. 3, pp. 118–125, Mar. 1988.

[3] T. Kawabata, T. Miyashita, and Y. Yamamoto, "Dead beat control of three phase PWM inverter," in *Proc. IEEE PESC'87*, 1987, pp. 473–481.

[4] K. P. Gokhale, A. Kawamura, and R. G. Hoft, "Dead beat microprocessor control of PWM inverter for sinusoidal output waveform synthesis," in *Proc. IEEE PESC'85*, 1985, pp. 28–36.

[5] A. Kawamura and K. Ishihara, "Real time digital feedback control of three phase PWM inverter with quick transient response suitable for uninterruptible power supply," in *Conf. Rec. IEEE-IAS Annu. Meeting*, 1988, pp. 728–734.

[6] M. Carpita and M. Marchesoni, "Experimental study of a power conditioning system using sliding mode control," *IEEE Trans. Power Electron.*, vol. 11, pp. 731–733, Sept. 1996.

[7] A. Kawamura and R. G. Hoft, "Instantaneous feedback controlled PWM inverter with adaptive hysteresis," *IEEE Trans. Ind. Applicat.*, vol. 20, pp. 769–775, July/Aug. 1984.

[8] T. Yokoyama and A. Kawamura, "Disturbance observer based fully digital controlled PWM inverter for CVCF operation," *IEEE Trans. Power Electron.*, vol. 9, pp. 473–480, Sept. 1994.

[9] S. L. Jung and Y. Y. Tzou, "Discrete sliding-mode control of a PWM inverter for sinusoidal output waveform with optimal sliding curve," *IEEE Trans. Power Electron.*, vol. 11, pp. 567–577, July 1996.

[10] T. Senjyu and K. Uezato, "Sinusoidal voltage controller for uninterruptible power supply by robust control," in *Proc. Power Conversion Conf.*, Yokohama, Japan, 1993, pp. 200–205.

[11] S. Muthu and J. M. S. Kim, "Discrete-time sliding mode control for output voltage regulation of three-phase voltage source inverters," in *Proc. IEEE APEC'98*, 1998, pp. 129–135.

[12] S. Hara, Y. Yamamoto, T. Omata, and M. Nakano, "Repetitive control system: A new type servo system for periodical exogenous signals," *IEEE Trans. Automat. Contr.*, vol. 33, pp. 659–667, July 1988.

[13] B. A. Francis and W. M. Wonham, "The internal model principle of control theory," *Automatica*, vol. 12, pp. 457–465, 1976.

[14] T. Inoue, "High accuracy control of servomechanism for repeated contouring," in *Proc. 10th Annu. Symp. Incremental Motion Control System and Devices*, 1981, pp. 258–292.

[15] M. Tomizuka, T. Tsao, and K. Chew, "Analysis and synthesis of discrete-time repetitive controllers," *Trans. ASME, J. Dyn. Syst. Meas. Control*, vol. 110, pp. 271–280, 1988.

[16] N. Sadegh, "A discrete-time MIMO repetitive controller," in *Proc. American Control Conf.*, 1992, pp. 2671–2675.
[17] C. Cosner, G. Anwar, and M. Tomizuka, "Plug in repetitive control for industrial robotic manipulators," in *Proc. IEEE Int. Conf. Robotics and Automation*, 1990, pp. 1970–1975.
[18] K. K. Chew and M. Tomizuka, "Digital control of repetitive errors in disk drive systems," in *Proc. American Control Conf.*, 1989, pp. 540–548.
[19] T. J. Manayathara, T. C. Tsao, J. Bentsman, and D. Ross, "Rejection of unknown periodic load disturbances in continuous steel casting process using learning repetitive control approach," *IEEE Trans. Contr. Syst. Technol.*, vol. 4, pp. 259–265, May 1996.
[20] H. L. Broberg and R. G. Molyet, "Correction of period errors in a weather satellite servo using repetitive control," in *Proc. 1st IEEE Conf. Control Applications*, Dayton, OH, Sept. 1992, pp. 682–683.
[21] T. Haneyoshi, A. Kawamura, and R. G. Hoft, "Waveform compensation of PWM inverter with cyclic fluctuating loads," in *Proc. IEEE PESC'87*, 1987, pp. 745–751.
[22] Y. Y. Tzou, R. S. Ou, S. L. Jung, and M. Y. Chang, "High-performance programmable ac power source with low harmonic distortion using DSP-based repetitive control technique," *IEEE Trans. Power Electron.*, vol. 12, pp. 715–725, July 1997.
[23] Y. Y. Tzou, S. L. Jung, and H. C. Yeh, "Adaptive repetitive control of PWM inverters for very low THD AC-voltage regulation with unknown loads," *IEEE Trans. Power Electron.*, vol. 14, pp. 973–981, Sept. 1999.
[24] M. Tomizuka, "Zero phase error tracking algorithm for digital control," *Trans. ASME, J. Dynam Syst. Meas. Control*, vol. 109, no. 2, pp. 65–68, 1987.
[25] H. L. Broberg and R. G. Molyet, "Reduction of repetitive errors in tracking of periodic signals: Theory and application of repetitive control," in *Proc. 1st IEEE Conf. Control Applications*, Dayton, OH, Sept. 1992, pp. 1116–1121.
[26] A. Kawamura and K. Ishihara, "Real time digital feedback control of three phase PWM inverter with quick transient response suitable for uninterruptible power supply," in *Conf. Rec. IEEE-IAS Annu. Meeting*, 1988, pp. 728–734.
[27] D. Wang, "On anticipatory iterative learning control design for continuous time nonlinear dynamic systems," in *Proc. IEEE Conf. Decision and Control*, Phoenix, AZ, Dec. 1999, pp. 1605–1610.

Keliang Zhou was born in Hubei, China, in 1970. He received the B.S. degree in applied electronics engineering from Huazhong University of Science and Technology, Wuhan, China, and the M.E.E. degree in electrical engineering from Wuhan University of Transportation, Wuhan, China, in 1992 and 1995, respectively. He is currently working toward the Ph.D. degree at Nanyang Technological University, Singapore.

His research interests are in the fields of power electronics and electric machines, advanced control theory, and applications.

Danwei Wang (S'88–M'89) received the B.E. degree from South China University of Technology, Guangzhou, China, and the M.S.E. and Ph.D. degrees from the University of Michigan, Ann Arbor, in 1982, 1985, and 1989, respectively.

Since 1989, he has been with the School of Electrical and Electronic Engineering, Nanyang Technological University, Singapore, where he is currently an Associate Professor and Deputy Director of the Robotics Research Center. His research interests include control theory and robotics. He has authored more than 100 published technical articles in the areas of iterative learning control and applications, manipulator/mobile robot dynamics, path planning, robust control, and adaptive control of such systems and position/force control systems.